Fxr1 regulates sleep and synaptic homeostasis

Jivan Khlghatyan[1,2], Alesya Evstratova[1], Lusine Bozoyan[1], Simon Chamberland[2,†], Aleksandra Marakhovskaia[1], Tiago Soares Silva[1], Katalin Toth[2], Valerie Mongrain[3], Jean-Martin Beaulieu[1,2*]

[1]Department of Pharmacology & Toxicology, University of Toronto, Medical Sciences Building, Toronto, ON M5S 1A8, Canada

[2]Department of Psychiatry and Neuroscience, Faculty of Medicine, Université Laval, Québec-City, QC G1J 2G3, Canada

[3]Department of Neuroscience, Université de Montréal and Center for Advanced Research in Sleep Medicine, Hôpital du Sacré-Coeur de Montréal, Montreal, QC H4J 1C5, Canada

†Now at: NYU Neuroscience Institute, New York University, Langone Medical Center, East River Science Park, New York, NY 10016, USA

*Correspondence to: martin.beaulieu@utoronto.ca

Abstract

Sleep homeostasis is a core mechanisms of sleep regulation. However, molecular substrates that modulate neuronal activity and plasticity during this process remains elusive. Homeostatic scaling mechanisms ensure stable net firing of neurons. Nevertheless, the involvement of scaling regulators in sleep homeostasis is unknown. By using Crispr/Cas9-mediated somatic knockouts, gene overexpression and monitoring of neuronal activity, we showed that the GWAS-identified insomnia and schizophrenia risk gene Fxr1 is engaged by scaling and sleep deprivation to controls AMPA receptors and synaptic strength. Regulation of Fxr1 under these conditions requires GSK3β. Furthermore, translatome sequencing revealed the engagement of local protein synthesis and synaptic structure associated transcripts by Fxr1 during sleep deprivation. Fxr1 may thus represent a molecular link between mental illnesses, homeostatic synaptic plasticity and sleep homeostasis.

One Sentence Summary

Homeostatic upscaling and sleep homeostasis engage a common regulator

Main Text

Sleep homeostasis that is the accumulation of sleep pressure during wake and dissipation during sleep is essential for brain physiology (*1*). Despite being a core regulatory component of sleep, the molecular mechanisms of sleep homeostasis remain elusive. Homeostatic synaptic scaling is a form of plasticity used by neurons to maintain net firing rates and is achieved by modulation of postsynaptic AMPA receptors (*2*). Certain molecular and structural changes involved in homeostatic scaling also occur during sleep (*3*, *4*). However, it is unclear whether molecular regulators of synaptic scaling are engaged during sleep homeostasis. Variants of the *FXR1* locus are GWAS-identified risk factors for insomnia (*5*) and are genetically linked to the duration of sleep (*6*). Fxr1 and Fxr2 are autosomal paralog of the fragile x mental retardation protein Fmr1. Among other functions, this family of RNA binding proteins has been shown to regulate AMPA receptors subunit synthesis (*7*) and Fmr1 has been involved in the regulation of synaptic scaling (*8*, *9*). We have used CRISPR/Cas9 and AAV mediated genetic manipulations *in vitro* and *in vivo*, EEG and whole cell recordings, and translatome sequencing to test the hypothesis that Fxr1 is a central modulator of synaptic scaling that is engaged in the regulation of sleep homeostasis.

We induced homeostatic upscaling (TTX) or downscaling (BIC) in primary cortical cultures. Protein levels of all Fxr1 isoforms decreased during upscaling (TTX vs Veh) (Fig. 1A) with no changes during downscaling (BIC vs Veh) (Fig. 1B). Fxr2 protein levels were also marginally decreased (Fig. S1A) while Fmr1 levels were not affected during upscaling (Fig. S1B). Upscaling did not affect mRNAs of Fxr1 and Fxr2 (Fig. S1C and D) and induced a slight increase of Fmr1 mRNA (Fig. S1E). This indicates that Fxr1 protein levels are strongly reduced during upscaling.

AMPA receptor surface expression is known to be modulated during homeostatic scaling (*10*). Neuronal cultures were infected with high efficiency by AAV SYN GFP-Fxr1 (Fxr1 over) or AAV SYN GFP (Ctrl) (Fig. S1F-H) followed by surface labeling for subunits of AMPA receptors. Surface expression of the GluA2 subunit did not change during upscaling or downscaling (Fig. S1I and K). Surface expression of GluA1 increased during upscaling in Ctrl (Ctrl TTX vs Ctrl Veh) and this increase was abolished by Fxr1 overexpression (Fxr1over TTX vs Fxr1over Veh) (Fig. 1C and D). Decrease of surface GluA1 during downscaling was similar in both Ctrl and Fxr1over conditions (Fig. 1C and D). No differences of surface GluA1 expression were observed between Ctrl Veh and Fxr1over Veh conditions (Fig. 1C and D). This indicates that augmentation of Fxr1 expression can specifically block the increase of surface GluA1 during upscaling.

To verify if Fxr1 negatively regulates GluA1 expression, we measured total protein levels of GluA1 by western blot in Ctrl and Fxr1over conditions during up or downscaling. Total GluA1 protein increased in Ctrl TTX condition compared to Ctrl Veh (Fig. S2A). This increase was not blocked but was rather exacerbated in Fxr1over condition (Fxr1overTTX vs Ctrl TTX) (Fig. S2A). We performed luciferase assays to address the effect of Fxr1 on GluA1 translation. Measurement of luciferase signal after expression of tagged luciferase cDNA (by 5'UTR or CDS or 3'UTR of GluA1) in Ctrl and Fxr1over conditions showed that Fxr1 can positively regulate the translation of GluA1 (Fig. S2C and D). No changes of total GluA1 protein during downscaling (Fig. S2B) or total GluA2 protein during upscaling (Fig. S1J) or downscaling (Fig. S1L) were observed. Overall, this suggests that augmentation of Fxr1 blocks increase of surface GluA1 during upscaling due to negative regulation of GluA1 transport to the surface of the plasma membrane.

We have previously shown that Gsk3β can negatively regulate Fxr1 protein levels (*11*). Upscaling resulted in an increase of Gsk3α and β activity (decrease in inhibitory phosphorylation) and decrease of Fxr1 protein (Fig. S3A-C). Conversely, inhibition of Gsk3 by lithium increased Fxr1 protein levels (Fig. S3A-C). This suggests the engagement of Gsk3 upstream of Fxr1 during upscaling. To address this, we designed *Fxr1* gene targeting guide RNAs (gRNAs) and validated these using Neuro2A cells (Fig. S3D-F). Then, the most efficient *Fxr1* targeting gRNA and a previously characterized *Gsk3b* targeting gRNA (*12*) were used to make CRISPR/Cas9 constructs to target Fxr1 and Gsk3β in neuronal cultures. All control plasmids contained scrambled gRNAs. We generated Fxr1KO and Fxr1Ctrl (both tagged with mCherry), Gsk3KO and Gsk3Ctrl (both tagged with GFP) constructs and performed low-efficiency transfection of neuronal cultures (Fig. S3G). Immunofluorescent staining revealed efficient single (Fxr1 or Gsk3β) or double (Gsk3β and Fxr1) knockouts of targeted genes (Fig. S3H-K). An expression vector encoding GFP-Fxr1 was used for overexpression of Fxr1 (Fxr1over) and a vector expressing GFP alone was used as a control (Ctrl). Whole cell patch clamp recordings showed a multiplicative increase in the mEPSC amplitude of control neurons following upscaling (Fig. 1E and J, Fig. S4A-C). Fxr1over or Gsk3KO prevented the increase of mEPSC amplitude induced by TTX (Fig. 1F,G and J). Fxr1KO resulted in an elevation of mEPSC amplitude (Fig. 1H and J) in a multiplicative manner (Fig. S4D-F) to a level that was not further increased following activity blockade by TTX (Fig. 1H and J). Gsk3/Fxr1KO also induced multiplicative elevation of mEPSC amplitude (Fig. 1I and J, Fig. S4G-I) that was not further increased by TTX treatment similar to Fxr1KO. No changes in mEPSC frequency were observed in all the conditions (Fig. S4J). Overall, this indicates that during upscaling Gsk3β is

activated and negatively regulates Fxr1 protein levels. In turn, the decrease in Fxr1 protein level is necessary and sufficient for upscaling.

Next, we investigated the impact of Fxr1 on sleep homeostasis. 48 hours of EEG and EMG recordings were performed in freely moving mice injected with AAV SYN GFP-Fxr1 (Fxr1over) or AAV SYN GFP (Ctrl) into the prefrontal cortex (PFC). Homeostatic sleep pressure accumulates during wake and is thus higher following enforced wakefulness or sleep deprivation (SD). We performed baseline (BL) recordings for 24h, followed by recordings during 6h of SD and 18h of recovery (REC). Measurement of the time spent in the wakefulness (WAKE), slow wave sleep (SWS) and paradoxical sleep (PS) indicated that Fxr1over mice have a significantly different distribution of vigilant states over time in BL, an effect that becomes more pronounced during the REC period (Fig. 2A, Fig. S5A). We computed the power spectra for WAKE, SWS and PS during BL and REC (Fig. 2B). When normalized to the Ctrl, we noticed significant differences in the alpha frequency band (8 to 11.75 Hz) during wakefulness only in the REC period (Fig. 2C and D). Pronounced effects during REC can be indicative of an involvement of Fxr1 in sleep homeostasis. SWS delta power increases with sleep pressure. Delta power further increases with SD, then it rapidly decreases during sleep followed by a rebound in early dark phase (*1*). Low alpha and high theta activity during WAKE was shown to drive the need for sleep (*13*). Moreover, decreased alpha/theta ratio is associated with daytime sleepiness (*14*). First, we found an increase in alpha/theta ratio of Fxr1over mice compared to controls starting from the onset of SD (Fig. 2E, Fig. S5B). Second, after SD, build-up of delta power in early dark phase was reduced in Fxr1over mice (Fig. 2F). This indicates an attenuation of SD effects in Fxr1over mice, which supports contributions to sleep homeostasis.

We thus investigated whether Fxr1 is engaged by SD. Western blot analysis showed decreased levels of Fxr1 in the PFC after SD (Fig. 3A, B). SD induced an increase in synaptic p845 GluA1 (Fig. 3C) with no changes for GluA2 (Fig. 3D). No changes of Fmr1 protein were found during SD (Fig. S6A). SD induced a slight increase in mRNA of Fxr2 (Fig. S6C) with no changes of Fxr1 or Fmr1 mRNAs (Fig. S6B,D).

To assess the effect of Fxr1 and its negative regulator Gsk3β on neuronal activity during SD, AAV SYN GFP-Fxr1 (Fxr1over), AAV Gsk3sgRNA/GFP + AAV SpCas9 (Gsk3sKO) (*12*), and AAV SYN GFP (Ctrl) were injected into mPFC three weeks prior to sleep deprivation. Whole cell patch clamp recordings on brain slices revealed that sleep deprivation increases mEPSC amplitude in control mice (Fig. 3E and H) in a non-multiplicative manner (Fig. S6E-H). This effect was completely abolished in Fxr1over and Gsk3sKO conditions (Fig. 3F-H). No changes were observed in mEPSC amplitude in all the conditions (Fig. S6I). Further characterization of the impact of SD on AMPA receptor functions revealed a reduction of the rectification index compatible with an increase of the GluA1/GluA2 subunits ratio in control mice (Fig. 3I and J). Conversely, this effect of sleep deprivation was again abolished in Fxr1over or Gsk3sKO conditions (Fig. 3I and J). This indicates that augmentation of Fxr1 can prevent the increase of synaptic GluA1 during sleep deprivation.

We then aimed to investigate the molecular signature of Fxr1 on sleep deprivation. As an RNA binding protein Fxr1 has a large number of targets (*15*), however, its neuronal targets are unknown. We used conditional RiboTag mediated RNA isolation (*16*) and translatome sequencing to find molecular targets that are engaged by both sleep deprivation and Fxr1. This approach allows to isolate ribosome-associated-RNAs only from cells that overexpress Fxr1. Moreover, unlike single cell or single nuclei techniques this approach provides a large amount of

mRNA with a better signal/noise ratio (*17*) and preserves dendritic mRNA, which is important for local translation during plasticity.

RiboTag mice (*16*) were infected with AAV SYN GFP-Fxr1 + AAV SYN Cre (Fxr1over) or AAV SYN GFP + AAV SYN Cre (Ctr) viruses three weeks prior to sleep deprivation (Fig. 4A). This allowed to activate RiboTag in the same neurons that overexpress Fxr1 (Fig. 4B and C). We found localization of GFP tagged Fxr1 along dendrites in close proximity with ribosomes (Fig. 4B) as previously reported (*18*). After sleep deprivation, RiboTag-associated-RNA was isolated and subjected to sequencing followed by pair wise comparison (Fig. 4A). We identified 2401 unique differentially expressed transcripts (DETs) in Ctrl/S vs Ctrl/SD comparison (Table S1). We then performed biological pathway enrichment (GO:BP) and clustering (Table S4). The top 10 clusters with the largest number of enriched pathways are shown in Fig. 4D. Five out of 10 clusters have relationship to the synapse (protein localization in synapse, synaptic vesicle transport, dendrite spine morphogenesis, transport along microtubule, junction substrate adhesion), thus we performed enrichment analysis using expert-curated and evidence-based synaptic gene ontology (SynGO) (*19*). This revealed that DETs engaged by sleep deprivation (Ctrl/S vs Ctrl/SD) are highly enriched in synaptic localizations, particularly in postsynapse (Fig. 4E, Table S6). Moreover, functional enrichment indicated involvement of those DETs in regulation of synapse organization, transport, metabolism and synaptic signaling (Fig. 4E, Table S6). Ctrl/SD vs Fxr1over/SD comparison identified 1626 unique DETs (Table S2). We found 241 unique transcripts that are affected by both SD and Fxr1 during SD (Fig 4F, Fig. S7, Table S3) (Ctrl/S vs Ctrl/SD overlap with Ctrl/SD vs Fxr1over/SD). For most transcripts (232) Fxr1 reversed changes induced by SD (e.g. upregulated by SD and downregulated by Fxr1 during SD) (Fig. S7A and B). These 232 transcripts were subjected to

further analysis, GO:BP enrichment and clustering revealed 4 pathways (dense core vesicle transport, microtubule polymerization, cytoplasmic translation, nucleosome DNA assembly) (Fig. 4G, Table S5). Localization analysis by SynGO identified enrichment in the postsynaptic compartments (Fig. 4H, Table S7). SynGO functional analysis showed enrichment in synapse organization and metabolism (Fig. 4H, Table S7). This shows that Fxr1 is involved in the regulation of synaptic processes such as local translation and regulation of synaptic structure (Fig. 4H) during SD.

Based on our findings, we propose the following model. During sleep deprivation or upscaling Fxr1 protein level decreases due to regulation by Gsk3β. Changes in Fxr1 protein induces alterations in synapse organization and metabolism, which subsequently affects synaptic GluA1 and postsynaptic excitatory activity. Fxr1 had no effect of basal neuronal activity *in vitro* and *in vivo*, it was not engaged by downscaling and did not affect baseline sleep. The regulatory function of Fxr1 was only engaged during the build-up of sleep pressure (during wake) and upscaling. This indicates the possible engagement of distinct molecular mechanisms of scaling based on sleep/wake state. Indeed, downscaling mechanisms are engaged during sleep (*3*). Moreover, upscaling mechanisms occurring as a result of visual deprivation are only engaged in the wake and are suppressed by sleep (*20*). Our study indicates that some molecular regulators of synaptic upscaling also operate during regulation of sleep homeostasis. Fxr1is GWAS-associated with schizophrenia and bipolar disorder (*21, 22*) and the regulation of emotional stability in humans (*11*). Expression of Fxr1 can be regulated by mood stabilizer drugs as a consequence of Gsk3 inhibition (*11*) and affects anxiety-related behaviors in mice (*12*). Neuropsychiatric disorders have been associated with misregulation of sleep (*23*) and homeostatic plasticity (*24*).

Thus, Fxr1 may represent a molecular link between mental illnesses, sleep homeostasis and homeostatic synaptic plasticity.

References and Notes:

1. G. M. Mang, P. Franken, Genetic dissection of sleep homeostasis. *Curr Top Behav Neurosci* **25**, 25-63 (2015).
2. G. G. Turrigiano, The self-tuning neuron: synaptic scaling of excitatory synapses. *Cell* **135**, 422-435 (2008).
3. G. H. Diering *et al.*, Homer1a drives homeostatic scaling-down of excitatory synapses during sleep. *Science* **355**, 511-515 (2017).
4. L. de Vivo *et al.*, Ultrastructural evidence for synaptic scaling across the wake/sleep cycle. *Science* **355**, 507-510 (2017).
5. P. R. Jansen *et al.*, Genome-wide analysis of insomnia in 1,331,010 individuals identifies new risk loci and functional pathways. *Nat Genet* **51**, 394-403 (2019).
6. H. S. Dashti *et al.*, Genome-wide association study identifies genetic loci for self-reported habitual sleep duration supported by accelerometer-derived estimates. *Nat Commun* **10**, 1100 (2019).
7. J. Khlghatyan, J. M. Beaulieu, Are FXR Family Proteins Integrators of Dopamine Signaling and Glutamatergic Neurotransmission in Mental Illnesses? *Front Synaptic Neurosci* **10**, 22 (2018).
8. M. E. Soden, L. Chen, Fragile X protein FMRP is required for homeostatic plasticity and regulation of synaptic strength by retinoic acid. *J Neurosci* **30**, 16910-16921 (2010).
9. K. Y. Lee, K. A. Jewett, H. J. Chung, N. P. Tsai, Loss of fragile X protein FMRP impairs homeostatic synaptic downscaling through tumor suppressor p53 and ubiquitin E3 ligase Nedd4-2. *Hum Mol Genet* **27**, 2805-2816 (2018).
10. G. H. Diering, A. S. Gustina, R. L. Huganir, PKA-GluA1 coupling via AKAP5 controls AMPA receptor phosphorylation and cell-surface targeting during bidirectional homeostatic plasticity. *Neuron* **84**, 790-805 (2014).
11. T. Del'Guidice *et al.*, FXR1P is a GSK3β substrate regulating mood and emotion processing. *Proc Natl Acad Sci U S A* **112**, E4610-4619 (2015).
12. J. Khlghatyan *et al.*, Mental Illnesses-Associated Fxr1 and Its Negative Regulator Gsk3β Are Modulators of Anxiety and Glutamatergic Neurotransmission. *Front Mol Neurosci* **11**, 119 (2018).
13. A. Vassalli, P. Franken, Hypocretin (orexin) is critical in sustaining theta/gamma-rich waking behaviors that drive sleep need. *Proc Natl Acad Sci U S A* **114**, E5464-E5473 (2017).
14. J. Cheung *et al.*, Increased EEG Theta Spectral Power in Sleep in Myotonic Dystrophy Type 1. *J Clin Sleep Med* **14**, 229-235 (2018).
15. M. Ascano *et al.*, FMRP targets distinct mRNA sequence elements to regulate protein expression. *Nature* **492**, 382-386 (2012).
16. E. Sanz *et al.*, Cell-type-specific isolation of ribosome-associated mRNA from complex tissues. *Proc Natl Acad Sci U S A* **106**, 13939-13944 (2009).
17. H. Kronman *et al.*, Biology and Bias in Cell Type-Specific RNAseq of Nucleus Accumbens Medium Spiny Neurons. *Sci Rep* **9**, 8350 (2019).

18. D. Cook *et al.*, Fragile X related protein 1 clusters with ribosomes and messenger RNAs at a subset of dendritic spines in the mouse hippocampus. *PLoS One* **6**, e26120 (2011).
19. F. Koopmans *et al.*, SynGO: An Evidence-Based, Expert-Curated Knowledge Base for the Synapse. *Neuron*, (2019).
20. K. B. Hengen, A. Torrado Pacheco, J. N. McGregor, S. D. Van Hooser, G. G. Turrigiano, Neuronal Firing Rate Homeostasis Is Inhibited by Sleep and Promoted by Wake. *Cell* **165**, 180-191 (2016).
21. S. W. G. o. t. P. G. Consortium, Biological insights from 108 schizophrenia-associated genetic loci. *Nature* **511**, 421-427 (2014).
22. X. Liu, J. R. Kelsoe, T. A. Greenwood, B. G. S. (BiGS), A genome-wide association study of bipolar disorder with comorbid eating disorder replicates the SOX2-OT region. *J Affect Disord* **189**, 141-149 (2016).
23. D. Picchioni, R. M. Reith, J. L. Nadel, C. B. Smith, Sleep, plasticity and the pathophysiology of neurodevelopmental disorders: the potential roles of protein synthesis and other cellular processes. *Brain Sci* **4**, 150-201 (2014).
24. J. Wondolowski, D. Dickman, Emerging links between homeostatic synaptic plasticity and neurological disease. *Front Cell Neurosci* **7**, 223 (2013).

Acknowledgments: Author acknowledge Chloé Provost and Julien Dufort-Gervais for technical help with AAV injection/EEG implantation surgery. **Funding:** JMB is Canada Research Chair in Molecular Psychiatry. VM is Canada Research Chair in Sleep Molecular Physiology. This work was supported by grants from Canada Institutes of Health Research (CIHR, PJT-148568) to JMB, and salary awards from CIHR and Fonds de recherche du Québec - Santé (FRQS) to VM. JMB is NARSAD independent investigator and One-Mind Rising Star awardee. **Author contributions:** JMB conceived the study. JMB and JK designed the experiments. JMB, JK, AE and VM wrote the manuscript. JK performed design and testing of CRISPR/Cas9 in vitro and in vivo, stereotaxic injections, protein expression analysis *in vitro* and *in vivo*, primary neuronal culture preparation, drug treatment and receptor surface staining and quantification, sleep deprivation, RiboTag IP and RNA extraction and RNAseq data analysis. AE and SC performed whole cell patch clamp recordings and data analysis. AM performed CRISPR/Cas9 KO experiments with puromycin selection followed by detection of Fxr1 expression. LB performed cloning and luciferase assay. VM performed EEG recordings and analysis. VM, AM and TSS participated in mouse sleep deprivation experiments. VM and KT provided technical, financial and intellectual support. **Competing interests:** Authors declare no conflict of interest. **Data and materials availability:** RNAseq data and analysis will be deposited to GEO. For additional materials please contact the lead author.

Supplementary Materials:

Materials and Methods

Figures S1-S7

Tables S1-S7

References (25-*34*)

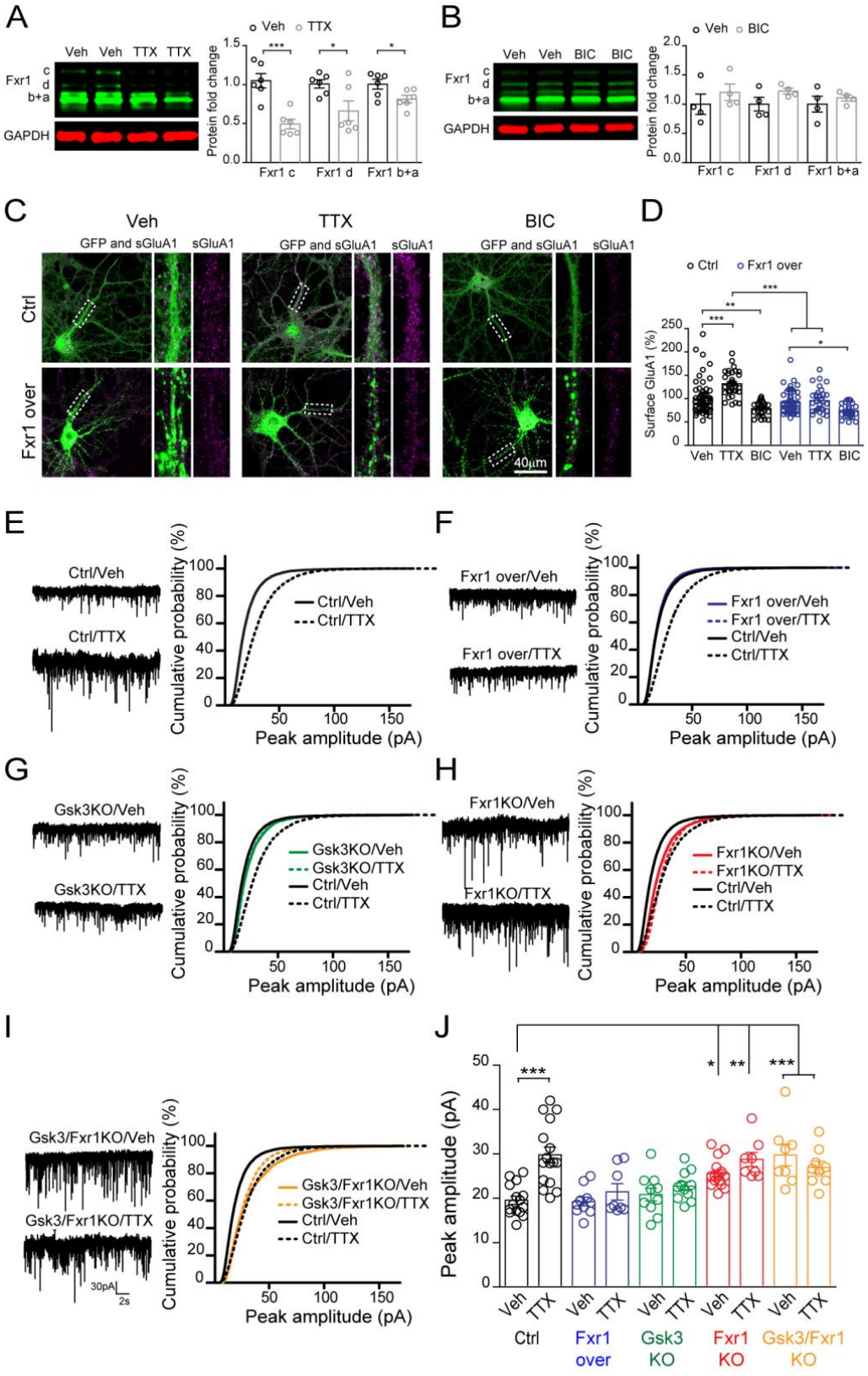

Fig. 1

Fig. 1. Fxr1 is a central component of homeostatic synaptic upscaling.

Western blot analysis of Fxr1 expression during (**A**) TTX induced upscaling (n=6 in each condition) and (**B**) BIC induced downscaling (n=4 in each condition) of primary postnatal cortical cultures. Student's T-test *p<0.05, ***p<0.001. (**C**) Immunostaining for surface GluA1 in GFP (Ctrl) or GFP-Fxr1 (Fxr1 over) infected cultures after treatment with Veh, TTX or BIC for 48h. (**D**) Percentage of surface GluA1 relative to the mean of Ctrl/Veh condition (Ctrl condition: Veh n=63, TTX n=34, BIC n=29, Fxr1over condition: Veh n=56, TTX n=30, BIC n=29). One way Anova with Bonferroni's Multiple Comparison Test *p<0.05, **p<0.01, ***p<0.001 (**E-I**) Cumulative probability plots of mEPSCs amplitude (500 events per cell) and representative examples of mEPSCs (left panel) recorded from cultured cortical neurons after 48 hours of 1 µM TTX or Veh exposure. (**E**) Control neurons (Ctrl/Veh n=16 and Ctrl/TTX n=17), (**F**) Fxr1P overexpressing neurons (Fxr1P over/Veh n=10 and Fxr1P over/TTX n=8), (**G**) Gsk3 KO neurons (Gsk3KO/Veh n=10 and Gsk3KO/TTX n=11), (**H**) Fxr1 KO neurons (Fxr1KO/Veh n=16 and Fxr1KO/TTX n=8), (**I**) Gsk3 and Fxr1 KO neurons (Gsk3/Fxr1KO/Veh n=8 and Gsk3/Fxr1KO/TTX n=11). (**J**) mEPSC amplitude of cultured cortical neurons after 48 hours of 1 µM TTX or Veh exposure. One way Anova with Bonferroni's Multiple Comparison Test *p<0.05, **p<0.01, ***p<0.001.

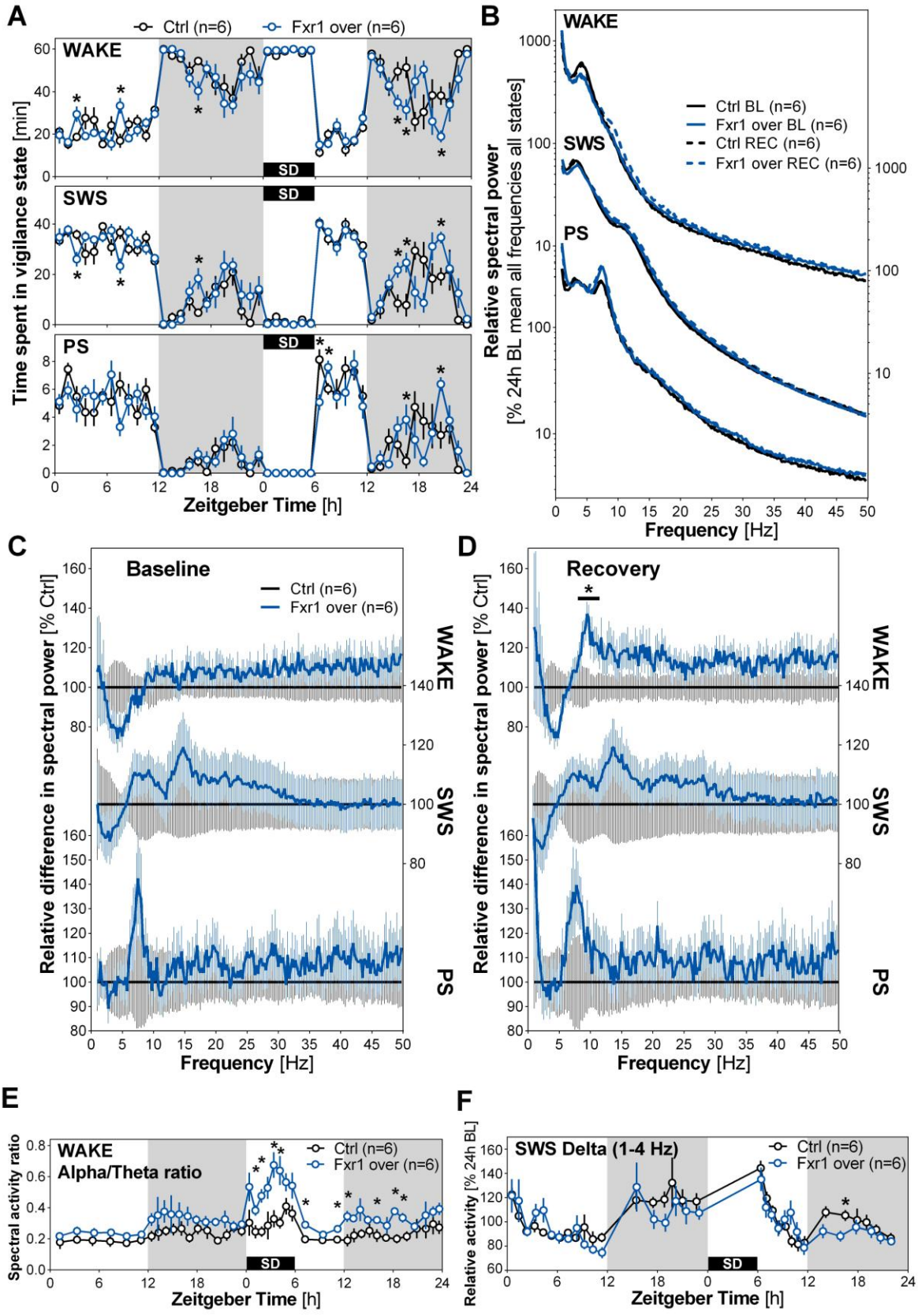

Fig. 2

Fig. 2. Fxr1 modulates sleep duration and recovery after sleep deprivation.

(**A**) Hourly distribution of wakefulness (WAKE), slow-wave sleep (SWS) and paradoxical sleep (PS) during a 24-h baseline (BL) recording and a second 24-h starting with a 6-h sleep deprivation (SD) (recovery: REC). Significant Group-by-Hour interactions were found for wakefulness during BL ($F_{23,230} = 1.67$) and REC ($F_{23,230} = 2.83$), for SWS during BL ($F_{23,230} = 1.66$) and REC ($F_{23,230} = 2.89$), and for PS during REC ($F_{16,160} = 2.54$). (**B**) Power spectra for WAKE, SWS and PS in Ctrl and Fxr1over mice computed between 0.75 and 50 Hz per 0.25-Hz for the full 24-h of BL and REC. (**C** and **D**) The spectral activity of Fxr1over mice expressed relative to that of Ctrl mice for WAKE, SWS and PS during (**C**) the 24-h BL and (**D**) the 24-h REC. A significant difference between groups was found for the frequency band 8 to 11.75 Hz during wakefulness ($t = 2.30$). (**E**) Time course of wakefulness spectral activity ratio between low alpha (8.5-10.5 Hz) and low theta (4-6 Hz) during BL and REC in Ctrl and Fxr1 over mice. A significant Group-by-Interval interaction was found for REC ($F_{22,220} = 1.96$). n=6 per group, Two-way ANOVA, Huynh-Feldt corrected, $^*p < 0.05$. (**F**) Time course of SWS delta activity during BL and REC in Ctrl and Fxr1over mice. A significant Group-by-Interval interaction was found during REC ($F_{13,130} = 1.89$). n=6 per group, Two way ANOVA, $^*p < 0.05$.

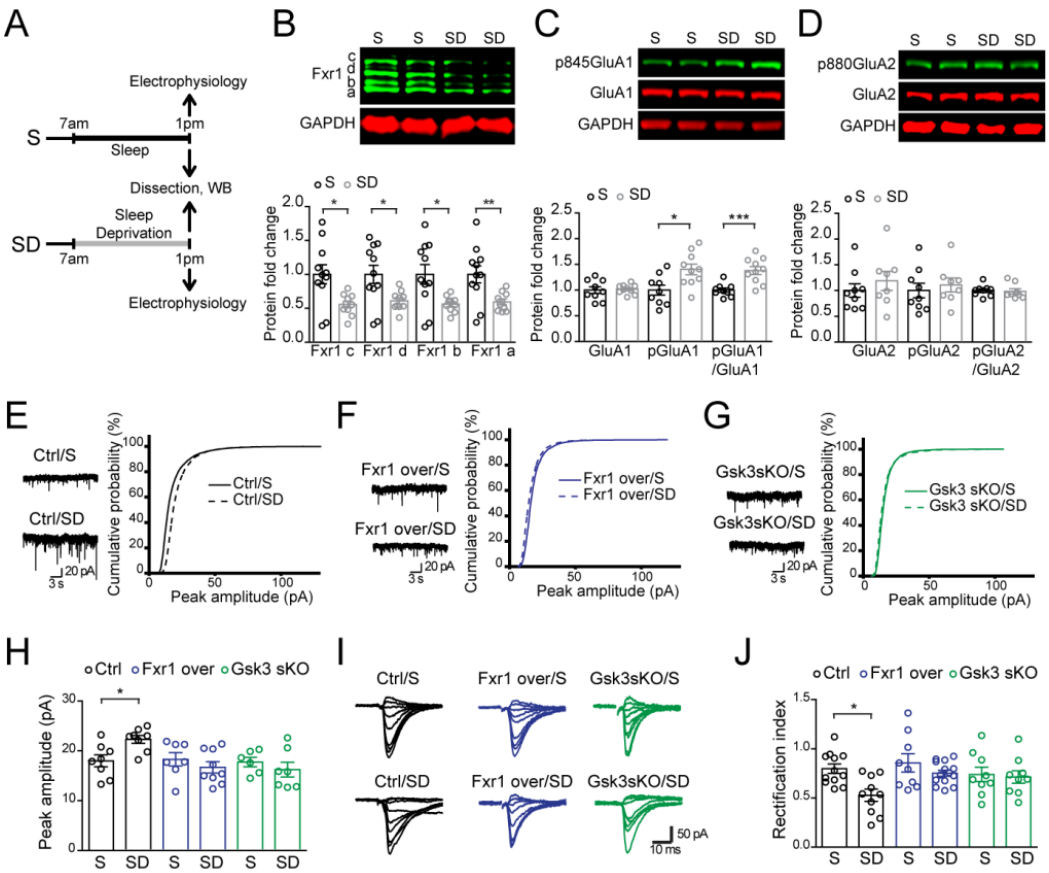

Fig. 3

Fig.3. Fxr1 regulates synaptic strength during sleep deprivation.

(**A**) Schematic representation of sleep deprivation experiments (**B-D**) Western blot analysis of (**B**) Fxr1 expression (S n=11, SD n=10), (**C**) p845GluA1 and GluA1 expression (S n=9, SD n=10), and (**D**) p880GluA2 and GluA2 expression (S n=9, SD n=8) in mPFC of sleeping and sleep deprived mice. Student's *t*-test $p < 0.05$, $^{**}p < 0.01$, $^{***}p < 0.001$ (**E-G**) Cumulative probability plots of mEPSCs amplitude (500 events per cell) and representative examples of mEPSCs (left panel) recorded from brain slices of S and SD mice. (**E**) Control neurons (Ctrl/S n=8, Ctrl/SD n=8), (**F**) Fxr1P overexpressing (Fxr1P over/S n=7, Fxr1P over/SD n=9), and (**G**) Gsk3sKO (Gsk3sKO/S n=6, Gsk3sKO/SD n=7) (**H**) mEPSC amplitude of cortical neurons of S or SD mice. (**I**) Representative examples of current-voltage relationship of evoked EPSC

amplitude recorded from S (top panel) and SD (bottom panel) mice. (**J**) Summary bar graphs showing rectification index of control (S n=12, and SD n=10), Fxr1P overexpressing (S n=9, and SD n=14) and Gsk3 sKO (S n=9, and SD n=9) neurons. One way ANOVA with Bonferroni's Multiple Comparison *$p < 0.05$.

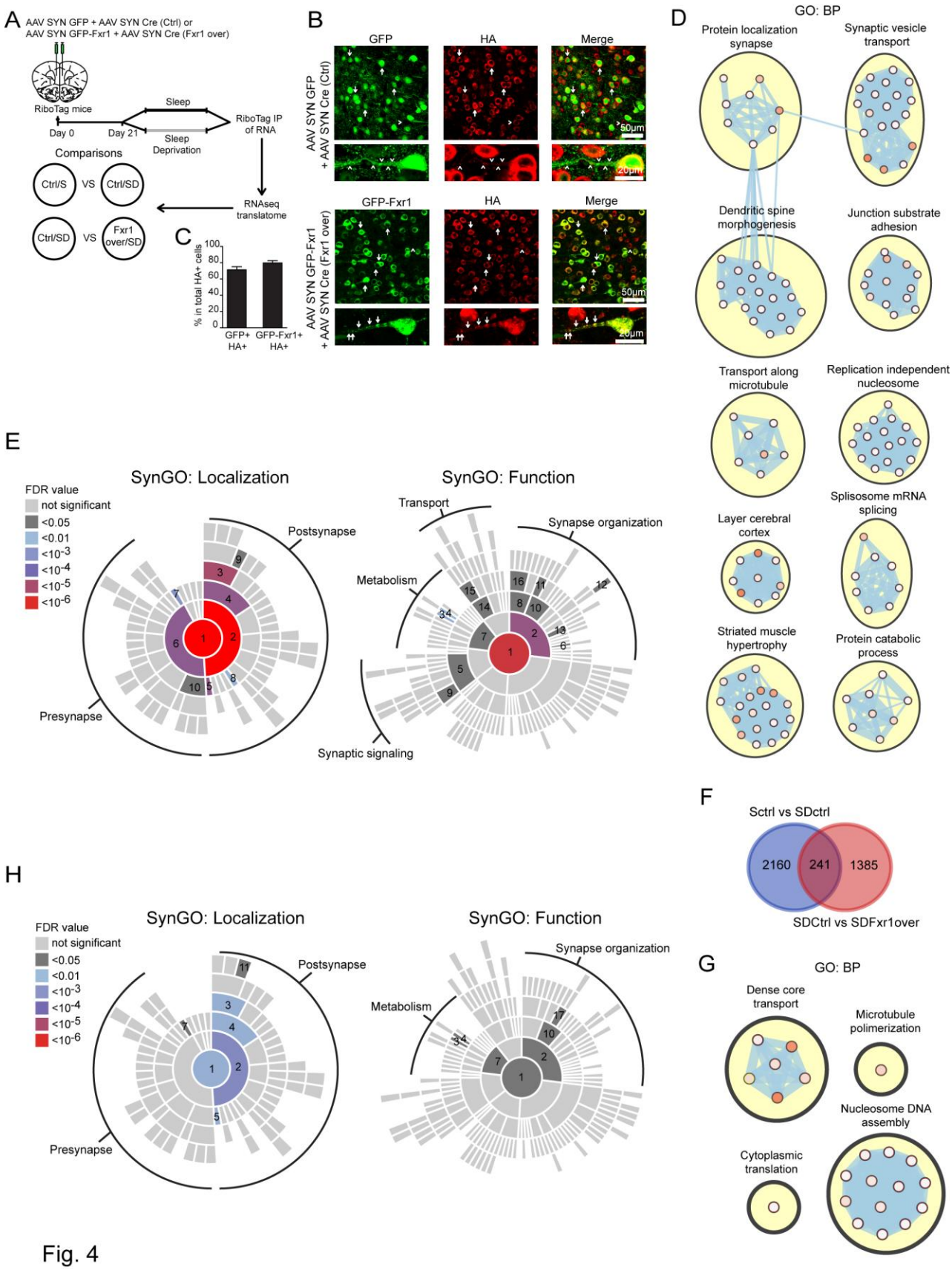

Fig. 4

Fig. 4. Neuronal translatome regulation by Fxr1 during sleep deprivation.

(**A**) Schematic representation of the experimental design. (**B**) Immunostaining for GFP and HA in Ctrl and Fxr1over mouse brain slices. Arrows indicate presence and arrowheads indicate absence of GFP tagged Fxr1 granules. (**C**) Quantification of colocalization of GFP and HA labeled neurons. (**D**) Enrichment of differentially expressed transcripts from Ctrl/S vs Ctrl/SD comparison in GO:BP. Top 10 clusters with the most number of enriched pathways (nodes) are shown. (**E**) SynGO enrichment for synaptic localization and function of differentially expressed transcripts from Ctrl/S vs Ctrl/SD comparison. (**F**) Venn diagram showing an overlap of differentially expressed transcripts between Ctrl/S vs Ctrl/SD and Ctrl/SD vs Fxr1over/SD comparisons. (**G**) Enrichment of commonly affected transcripts between Ctrl/S vs Ctrl/SD and Ctrl/SD vs Fxr1over/SD comparisons in GO:BP. (**H**) SynGO enrichment for synaptic localization and function of common affected transcripts between Ctrl/S vs Ctrl/SD and Ctrl/SD vs Fxr1over/SD comparisons.

SynGO Localization: 1-Synapse, 2-Postsynapse, 3-Postsynaptic density, 4-Postsynaptic specialization, 5-Postsynaptic ribosome, 6-Presynapse, 7-Presynaptic ribosome, 8-Postsynaptic cytosol, 9-Postsynaptic density intracellular compartment, 10-Presynaptic active zone, 11-Integral component of postsynaptic density membrane.

SynGO function: 1-Process in the synapse, 2-Synapse organization, 3-Protein translation at presynapse, 4-Protein translation at postsynapse, 5-Trans-synaptic signaling, 6-Synapse adhesion between pre- and post-synapse, 7-Metabolism, 8-Structural constituent of synapse, 9-Chemical synaptic transmission, 10-Synapse assembly, 11-Regulation of synapse assembly, 12-Regulation of modification of postsynaptic actin cytoskeleton, 13-Postsynaptic cytoskeleton organization,

14-Axo-dendritic transport, 15-Dendritic transport, 16-Structural constituent of postsynapse, 17-Postsynaptic specialization assembly.